CONF-8703116--3

ELECTRON TRANSFER PROCESSES IN COLLISIONS OF HIGHLY CHARGED ENERGETIC (0.1 to 1.0 MeV/Nucleon) IONS WITH HELIUM ATOMS[†]

S. Datz, R. Hippler[*], L. H. Andersen[+], P. F. Dittner, H. Knudsen[+],
H. F. Krause, P. D. Miller, P. L. Pepmiller, T. Rosseel,
N. Stolterfoht,[#] and Y. Yamazaki[§]

Oak Ridge National Laboratory, Oak Ridge, TN 37831, U.S.A.

CONF-8703116--3

DE87 008808

Abstract

We have investigated charge transfer in collisions of energetic (0.1 - 1 MeV/nucleon) highly charged ions with helium atoms with the principal aim of clarifying the nature of two-electron processes. The sensitivity of partial charge-changing cross sections (i.e., single- and double-charge transfer, transfer ionization (TI), and single and double ionization) to core configuration and scaling rules for one- and two-electron processs were investigated with iodine ions (q = 5+ → 26+) and uranium ions (q = 17+ → 44+) using an ion-charge state, recoil-ion coincidence method. Using zero-degree electron spectroscopy in coincidence with charge transfer, we found that at the higher energies, as in the case of 0.1 MeV/nucleon ions previously reported, TI involves the transfer of two electrons to a higher correlated state followed by loss of one electron to the continuum. In addition, we observe very high Rydberg electrons in coincidence with TI, implying a possible up-down correlation in the pair transfer. In addition, we made measurements of VUV photons emitted at the collision in coincidence with He^+ and He^{2+} recoils. The results show that TI leads to capture into lower n states than single-charge transfer.

[†] Research was sponsored by the U.S. Department of Energy, Division of Chemical Sciences under Contract No. DE-AC05-84OR21400 with Martin Marietta Energy Systems, Inc.

DISCLAIMER

1. Introduction

The interactions of bound electrons with the strong Coulomb field supplied by an oncoming highly charged ion have been subjects of considerable study at several laboratories in recent years. If the ion is of sufficiently high charge, the binding energy match with the electrons in the outer shell of a neutral taget atom is such that transfer should take place to high lying n states of the projectile ion. It has been assumed that for sufficiently high n states, the core configuration of the ion should not be of much consequence so that the collision physics of an ion of charge, q, should be equivalent to that of a bare nucleus of charge Z equal to q. This is a particular convenient assumption since it permits great simplification in the theoretical treatment of charge transfer. A test of this assumption is one of the goals of this paper.

The large field supplied by the highly charged ions also gives rise to large release distances and the possibility of more than one electron being involved in inelastic collision processes such as charge transfer and ionization. Satisfactory scaling rules relating single electron capture and ionization cross sections to ion charge and velocity have been developed, but for two electron processes, there is a paucity of data and tests of existing scaling rules are needed. This is the second objective of this paper.

In previous experiments [1], it has been shown, though the utilization of zero degree electron spectroscopy, that transfer ionization in collisions of Au^{q+} ions on He at 0.1 MeV/nucleon involves the transfer of two electrons from the helium to the gold followed by the emission of one electron into an apparent energy continuum. This observation suggested that two electron transfer occurs as a correlated pair. It is desirable to extend these measurements to higher velocities (and charge states) to see if one can observe a transition to independent particle behavior. This is the third objective of this paper.

Finally, we inquire as to the fate of the electron which remains behind on the highly charged core in the transfer ionization process, i.e., what is the n state distribution for these electrons compared with the distribution for single-electron transfer? To answer this question, we carried out experiments in which we measured ion charge states in coincidence with VUV photons.

2. Core state dependence of charge transfer cross sections

To test the assumption of core state independence, we used a helium atom target and ions of ${}^{127}\mathrm{I}_{53}^{q+}$ at 100 keV/nucleon (q = 5 → 16) and 250 keV/nucleon (q = 9 → 26) ${}^{238}\mathrm{U}_{92}^{q+}$ a 250 keV/nucleon (q = 17 → 30), 500 keV/nucleon (q = 23 → 37), and 1000 keV/nucleon (q = 26 → 44). The U^{q+} and I^{q+} data can be intercompared at 250 keV/nucleon. The 100 keV/nucleon ${}^{127}\mathrm{I}_{53}^{q+}$ data may be compared with similar data on ${}^{197}\mathrm{Au}_{79}^{q+}$ at 100 keV/nucleon taken in earlier experiments at Aarhus University [2].

A schematic of the experimental setup is shown in Fig. 1. Beams of ${}^{127}\mathrm{I}_{53}^{q+}$ at 12.7 MeV (100 keV/nucleon) and 31.75 MeV (250 keV/nucleon) obtained from the ORNL EN Tandem Facility and beams of ${}^{238}\mathrm{U}_{92}^{q+}$ at 59.5 MeV (0.25 MeV/nucleon), 119 MeV (0.5 MeV/nucleon), and 238 MeV (1.0 MeV/nucleon) obtained from the Holifield Heavy Ion Research Facility (HHIRF) were post stripped in a carbon foil to obtain an array of charge states. A given charge state, q, was magnetically selected and passed through a windowless gas cell containing He. The beam then continued through an electrostatic analyzer and the charge dispersed beam struck a solid-state position-sensitive detector (PSD). Because of the high charge states achieved by foil stripping, the cross section for further ionization of the projectile were small and the charge states recorded on the PSD were the initial charge, q, and charges q-1 and q-2. The helium ions He^+ and He^{++} created in the gas cell were accelerated out of the collision region, drifted across an ~10 cm space and impinged upon a channel-plate electron multiplier. The arrival of a helium ion at the channel plate started a time-to-amplitude converter (TAC). The stop pulse was supplied by the arrival of an ion at the PSD. The time delay for a coincidence was dependent on the time-of-flight of the helium ion; i.e., a He^{++} ion, having received twice the energy as a He^+ ion, spans the drift space in less time ($1/\sqrt{2}$) than He^+.

The result is an array in a two-dimensional spectrum. Following the convention of Damsgaard et al. [2], we denote a given partial cross section according to initial and final charges of the He as a superscript and the multicharged ion as a subscript. We obtain from our array; $\sigma^{01}_{q,q}$ single ionization, σ^{02}_{qq} double ionization, $\sigma^{01}_{q,q-1}$ single charge transfer, $\sigma^{02}_{q,q-1}$ transfer ionization, and $\sigma^{02}_{q,q-2}$ double electron capture. (Pulses obtained in "$\sigma^{01}_{q,q-2}$" channel are obviously spurious and are a measure of beam charge state impurity and double collisions in the gas cell.)

In fig. 2, we show a comparison of the cross sections obtained in the present experiment with 100 keV/nucleon ${}^{127}I^{q+}_{53}$ to those obtained by Damsgaard et al. at Aarhus for 100 keV/nucleon ${}^{198}Au^{q+}_{79}$ ions, and in fig. 3 a similar comparison is made between our results for ${}^{238}U^{q+}_{92}$ and ${}^{127}I^{q+}_{53}$ at

250 keV/nucleon. The cross sections obtained for the uranium-helium system are displayed in figs. 4, 5 and 6 ($^{238}U^{q+}_{92}$ 250 keV/nucleon, 500 keV/nucleon, and 1000 keV/nucleon, respectively).

In the main, the scaling of all the cross sections with charge state as shown in figs. 2 and 3 is quite close; the I-U scaling being somewhat closer than that for the I-Au system. Deviations from exact charge-state scaling in total-single capture cross sections, $\sigma_{q,q-1} = \sigma^{01}_{q,q-1} + \sigma^{02}_{q,q-1}$, for 100 keV/nucleon Dy^{q+}, Ta^{q+}, Re^{q+}, Au^{q+}, and U^{q+} collisions with hydrogen molecules was demonstrated by Hvelplund et al. [3] who found deviations of order ±50% from theoretical estimates based on the Bohr-Lindhard theory [4]. Although significant variations in the total single-capture cross sections at these velocities have been well documented, the reasons are still not well understood. There does seem to be a consistent depression of about a factor of two in the capture cross section at certain closed shell configurations as first noted by Datz et al. [5] for Br^{7+} ($3d^{10}$). This depression appears in the present data for I^{7+}($4d^{10}$), for U^{24+}($5p^6$), and in the Aarhus data for the $5p^6$ configuration at Au^{11+}. Surprisingly, the largest deviations (i.e., factors of ~2) are in the single-ionization cross sections of He by Au and by I shown in fig. 2. Since all the partial cross sections are obtained simultaneously in the present experiment, the close agreement of the other partial cross sections of fig. 2 precludes the possibility of systematic experimental differences between the Oak Ridge I^{q+} data and the Aarhus Au^{q+} data. Theoretical calculations of McDowell and Janev[6] agree closely with our I^{q+} data.

For all the data from 250 keV/nucleon up (see figs. 4-6), the single-ionization cross sections are exceedingly flat with both energy and charge; the maximum change is a factor of less than 2 over the entire measured range. This result is in accord with expectations since for all the collisions studied in this paper the Bohr parameter $\kappa = 2q(v_0/v)$ where v_0 is the Bohr velocity and v is the ion velocity [7] is much greater than unity. The ratio between double and single ionization of He using bare ions up to O^{8+} has been measured by Knudsen et al. [8] at small values of $\kappa = 2q\,(v_0/v)$. The ratio was shown to be linear when plotted versus $q^2/(E \ln (13.123\sqrt{E}))$. A similar plot for our data shows no consistency at all; in all cases our $\kappa > 1$ and the theory of ref. [8] should not fit. Instead, we find a remarkably constant ratio of about 1:3 at energies of 500 to 1000 keV/nucleon.

In fig. 7, we plot the total-capture cross section $\sigma_{q,q-1} = \sigma^{01}_{q,q-1} + \sigma^{02}_{q,q-1}$ versus E(keV/nucleon)$q^{4/7}$ for all energy and charge ranges measured. The dashed curve is the universal scaling curve for highly charged ion-helium atom collisions developed by Knudsen [9]. It is seen to fit $\sigma_{q,q-1}$ reasonably well, the maximum deviation being only a factor of two. More interesting is the variation in the ratio of transfer ionization $\sigma^{02}_{q,q-1}$ to $\sigma^{01}_{q,q-1}$ which increases from ~0.5 at 100 keV/nucleon to almost 3 at 1000 keV/nucleon. Aside from the shell effect on capture cross section (i.e., dips at I^{7+} (at 100 keV/nucleon) and U^{24+} (at 250 keV/nucleon)) there is also reasonably good scaling for the separate partial cross sections. Another scaling has been suggested by Tanis et al. [10], who proposed that the ratio $(R + 1) = (\sigma^{01}_{q,q-1} + \sigma^{02}_{q,q-1}) / \sigma^{02}_{q,q-1}$ should scale with $(E/\text{nucleon})^{1/2}/q$. From a number of measurements, they derive a semi-empirical relationship

$$(R + 1) \approx 40 / E^{0.3} \times q^{0.4} \quad .$$

In fig. 8, we plot our data in this reference frame. The predicted value is shown by the line and agrees quite well with the data. The theory, however, is not very sensitive in this region as can be shown by simply letting $R = 0$, thereby eliminating all the physics. The result with this assumption for $E = 1000$ keV/nucleon, shown as a dashed line, is in even better agreement with the data.

3. Zero degree electron spectroscopy study of transfer ionization

The objective here is to probe the nature of transfer ionization. Does it consist of two independent events or is there strong correlation between the two electrons lost from the helium? Is one electron captured to a bound state and the second electron liberated in the rest frame of the He? Or is the second electron captured to a continuum state of the heavy ion? Or are two electrons captured to an autoionizing state of the heavy ion leaving a single electron in a bound state. From previous experiments on zero-degree electron spectroscopy with Au^{q+} at 100 keV/nucleon [1], it would appear that the answer is .... none of the above. A question is whether the behavior will become more independent particle-like at higher velocities.

The present experiment utilized U^{q+} beams from the HHIRF. The beams passed through a windowless gas cell into a tandem electrostatic analyzer [11] (TESA) and then into an ion-charge state analyzer (as in fig. 1). The electrons, after passing through the first half of the TESA can be decelerated before passing through the second half, thereby inproving the resolution of the system.

Electron spectra were taken in coincidence with the initial charge state q and in coincidence with charge capture at q-1. Since we use He as a target, coincidence of a free electron with a transferred electron implies transfer ionization to form He^{++}. The resultant spectra for U^{30+} at 500 keV/nucleon are shown in fig. 9. As before [1], the singles spectrum displays a continuum peak with symmetrically placed satellites due to forward and backward emission of electrons from autoionizing states. An additional feature is the peak on the high energy side of the cusp which is due to Rydberg electrons stripped from the ion by the field in the elecrostatic analyzer. (These electrons are made observable in the present experiment because of the use of the deceleration field between the two halves of the TESA.) The maximum n state which can remain bound to an ion in the electrostatic field is given by

$$n_{max} \cong (6.3 \times 10^8 q^3/E)^{1/4}$$

where q is the core charge and E is the field in volts per cm. For the field of ~100 V/cm of the TESA and a charge $q = 30+$, this means that the stripped electrons were bound into states $n > 600$.

The coincidence spectra 9b and 9c behave in much the same way as the ones taken at the lower velocity [1]. The q → q coincidences display a capture to continuum peak bounded by autoionization electrons which arise from electron transfer plus core excitation followed by re-emission.

The q → q-1 coincidence (tranfer ionization) spectrum contains no autoionizing peaks and, when unfolded into the rest frame of the projectile, gives a symmetric flat forward-backward distribution characteristic of electron loss to the continuum and <u>not</u> electron capture to the continuum. Thus, even at this higher velocity, we propose that we can account for transfer ionization by the transfer of two electrons to a highly correlated state on the U projectile followed by the loss of one electron to the continuum. (Discussions of this point can be found in refs. [1, 11 and 12]. A new feature here is the Rydberg peak which appears in the transfer ionization spectrum. This result is related to the observation of loss to continuum electrons near zero energy, i.e., these electrons lie just below the continuum; for n = 600 the binding energy is just ~30 meV. If the second electron lies below $n \cong 600$, it might be Stark stripped in the electrostatic charge-state analyzer where we have fields of $\sim 10^4$ volts/cm. In this case, $n_{max} \simeq 200$ so that for $200 < n < 600$ the second electron would be lost, the ion would appear at q-1 but with no coincident electron. For $n < 200$, the ion would be stable to stripping and would appear at q-2, but we know that double capture is orders of magnitude lower than transfer ionization. Therefore, the second electron must be transferred to a high n state close to the continuum. This is suggestive of a similar result which has recently been found at lower energies,[14,15] where electron pair transfer from He to, e.g., O^{6+} at lower energies leads to a high probability of one electron going to a low n state ($n = 2$) and the second to a high $n > 5$ state rather than both going to $n = 3$.

4. n State populations in transfer ionization

It may be inferred from the results above that the electron pair transfer On these collisions takes place to poorly defined states. However, once one of the electrons leaves, the state of the remaining electron must be well defined. The idea for this part of the experiment then is to compare the n distribution for simple single charge transfer with that obtained from transfer ionization. In principal, this could be done via an experiment in which we measured a photon emission spectrum from a (q-1) ion in coincidence with He^+ recoil (simple charge transfer) and He^{++} (transfer ionization). In practice, this is exceedingly difficult because of the low collection and detection efficiency of spectrometers especially since the photons in question lie in the VUV.

Instead, we did the following experiment. Immediately opposite the recoil ion collector of fig. 2, we placed some VUV photon filters and detectors and measured the ratio of photons collected in these bands in coincidence with He^+ and He^{++}. Knowing the relative cross sections for the formation of He^+ and He^{++}, we can make a comparison of photon yields per ion formed. For this experiment we used I^{17+} at 100 keV/nucleon where competing processes for making He^+ and He^{++} in coincidence with an excited iodine ionic state should be small (see fig. 10). For VUV filter-detector systems, we used an Al:Si/Ti filter coupled with channeltron which is sensitive in the range 16-22 nm and 35-50 nm, and a supramil filter coupled with an EMR 541 G-X photomultiplier which is sensitive in the 160-200 nm range. These ranges correspond to $n = 6 \rightarrow 5$ (43 nm) and $n = 10 \rightarrow 9$ (182 nm) transitions respectively for the I^{17+} ion core. In fig. 10, we plot the theoretical prediction of McDowell and Janev [6] for the normalized n distribution in single charge transfer from He to a 17+ ion at 100 keV/nucleon. And at $n = 6$ and $n = 10$, we plot the fraction of photons obtained in coincidence with transfer ionization at these n states; i.e., a factor of about 0.1 at $n = 10$ and about 0.5 at $n = 6$. Since these are normalized, the implication is that transfer ionization leads to lower n states than simple single charge transfer.

References

* Present address: Universität Bielefeld, Fakultät für Physik, Postfach 8640, 4800 Bielefeld 1, F.R.G.

\+ Present address: Institute of Physics, University of Aarhus, DK-8000, Aarhus C, Denmark.

Present address: Hahn-Meitner-Institut für Kernforschung Berlin GmbH, Bereich Kern-und Strahlenphysik, D 1000 Berlin 39, F.R.G.

§ Present address: Research Laboratory for Nuclear Reactors, Tokyo Institute of Technology, Tokyo, Japan.

1. L. H. Andersen, M. Frost, P. Hvelplund, H. Knudsen, and S. Datz, Phys. Rev. Lett. 52 (1984) 518.
2. H. Damsgaard, H. K. Haugen, P. Hvelplund, and H. Knudsen, Phys. Rev. A27 (1983) 112.
3. P. Hvelplund, H. Knudsen, L. H. Andersen, S. K. Bjornluvd, and L. Liljeby, Abstracts of the XIII Int. Conf. on the Physics of Electronic and Atomic Collisions, J. Eichler et al., eds., ICPEAC Berlin (1983) p. 564.
4. P. Hvelplund and A. Andersen, Phys. Scripta 26 (1983) 375.
5. S. Datz, H. O. Lutz, L. B. Bridwell, C. D. Moak, H. D. Betz, and L. D. Ellsworth, Phys. Rev. A2 (1970) 430.
6. M.R.C. McDowell and R. K. Janev, J. Phys. B: At. Mol. Phys. 17 (1984) 2295.
7. H. Knudsen, Physics of Electronic and Atomic Collision, S. Datz, ed., North-Holland Press (1982), pp. 657-671.
8. H. Knudsen, L. H. Andersen, P. Hvelplund, G. Astner, H. Cedarquist, H. Danared, L. Liljeby, and K. G. Rensfelt, Abstracts XIII ICPEAC, J. Eichler et al., eds., Berlin (1983), p. 416.
9. H. Knudsen, H. K. Haugen, and P. Hvelplund, Phys. Rev. A23 (1981) 597.
10. J. A. Tanis, M. W. Clark, R. Price, S. M. Ferguson, and R. E. Olson, Proc., Conf. on Physics of Multiply Charged Ions, Groningen, The Netherlands, Sept. 1986, in press.
11. A. Itoh, T. Schneider, G. Schiwietz, H. Platten, G. Nolte, D. Schneider, and N. Stolterfoht, J. Phys. B 16 (1983) 3965; A. Itoh, D. Schneider, T. Schneider, T.J.M. Zouros, G. Nolte, G. Schiwietz, W. Zeitz, and N. Stolterfoht, Phys. Rev. 31 (1985) 684.

References (contd)

12. S. Datz, C. Bottcher, L. H. Andersen, P. Hvelplund, and H. Knudsen, Nucl. Instr. Meth. Phys. Res. B10/11 (1985) 116.

13. L. H. Andersen, M. Frost, P. Hvelplund, and H. Knudsen, J. Phys. B: At. Mol. Phys. 17 (1984) 4701.

14. N. Stolterfoht, C. C. Havener, R. A. Phaneuf, J. K. Swenson, S. M. Shafroth, and F. W. Meyer, Phys. Rev. Lett. 57 (1986) 74.

15. R. Mann and H. Schulte, Z. Phys. D 4 (1987) 343.

Figure Captions

Fig. 1. Schematic of apparatus for measurement of partial cross sections.

Fig. 2. Partial charge-changing cross sections for I^{q+} at 100 keV/nucleon (Δ) and Au^{q+} at 100 keV/nucleon ([]) from ref. 2.

Fig. 3. Partial charge-changing cross sections for I^{q+} at 250 keV/nucleon (Δ) and U^{q+} at 250 keV/nucleon ([]).

Fig. 4. Partial charge-changing cross sections for U^{q+} at 250 keV/nucleon $o = \sigma^{01}_{q,q}$, $\bullet = \sigma^{02}_{q,q}$, $\Delta = \sigma^{01}_{q,q-1}$, $\Delta = \sigma^{02}_{q,q-1}$, $[] = \sigma^{02}_{q,q-2}$.

Fig. 5. Partial charge-changing cross sections for U^{q+} at 500 keV/nucleon $o = \sigma^{01}_{q,q}$, $\bullet = \sigma^{02}_{q,q}$, $\Delta = \sigma^{01}_{q,q-1}$, $\Delta = \sigma^{02}_{q,q-1}$.

Fig. 6. Partial charge-changing cross sections for U^{q+} at 1000 keV/nucleon $o = \sigma^{01}_{q,q}$, $\bullet = \sigma^{02}_{q,q}$, $\Delta = \sigma^{01}_{q,q-1}$, $\Delta = \sigma^{02}_{q,q-1}$.

Fig. 7. $(\sigma_{q,q-1})/q$, $(\sigma^{01}_{q,q-1})/q$, and $(\sigma^{02}_{q,q-1}/q)$ versus E (keV/nucleon)/$q^{4/7}$; dashed line is theory for $(\sigma_{q,q-1})/q$ from ref. 9.

Fig. 8. Ratio, R, of $\sigma^{01}_{q,q-1}$ to $\sigma^{02}_{q,q-1}$. Solid line is from semi-empirical theory of Tanis et al. [ref. 10]. The dashed line simply assumes R = 0 at 1000 keV/nucleon.

Fig. 9. Zero-degree electron spectra taken for U^{30+} at 500 keV/nucleon passing through a He target. (a) Singles spectrum, (b) coincidence with exit charge state 30+, and (c) coincidence with exit charge state 29+.

Figure Captions (contd)

Fig. 10. Normalized distribution of $\sigma^{01}_{q,q-1}(n)$ versus *n* for a 100 keV/nucleon charge 17+ ion capturing from He(●) from ref. 6. The remaining two points represent the measured corresponding values for $\sigma^{02}_{q,q-1}(o)$.

ORNL—DWG 86—18201

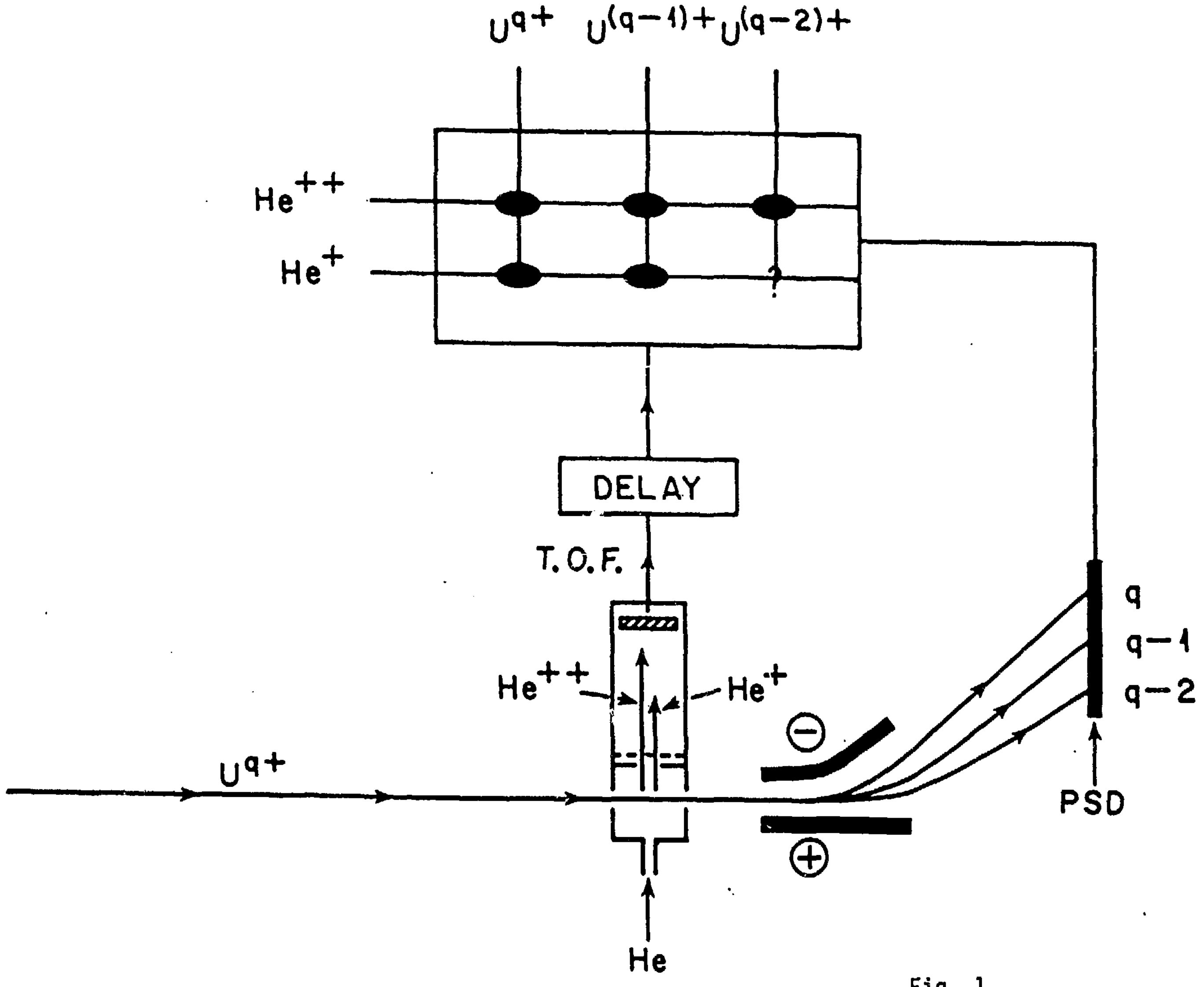

Fig. 1

ORNL–DWG 86–18202

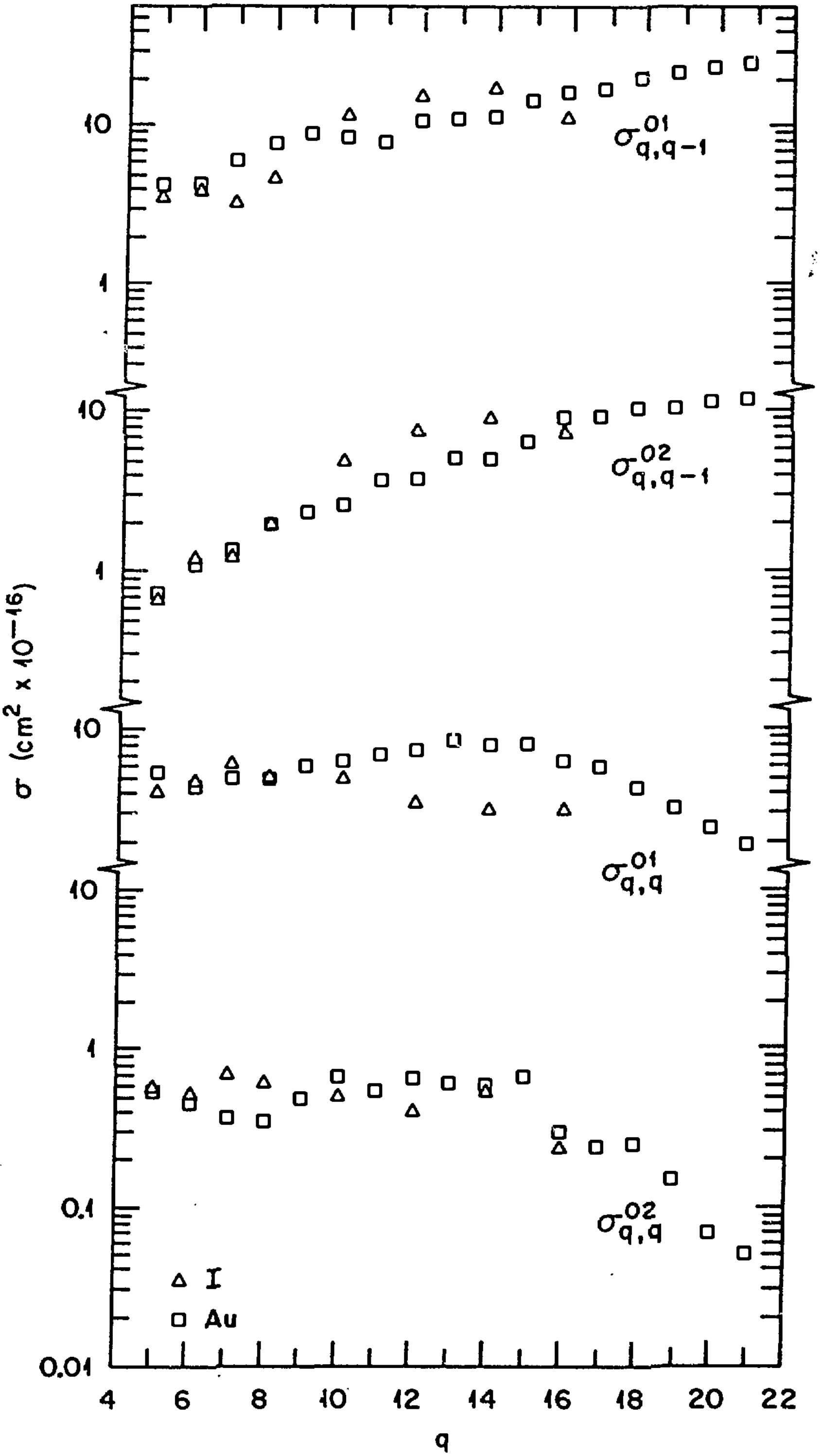

Fig. 2

ORNL—DWG 86—48203

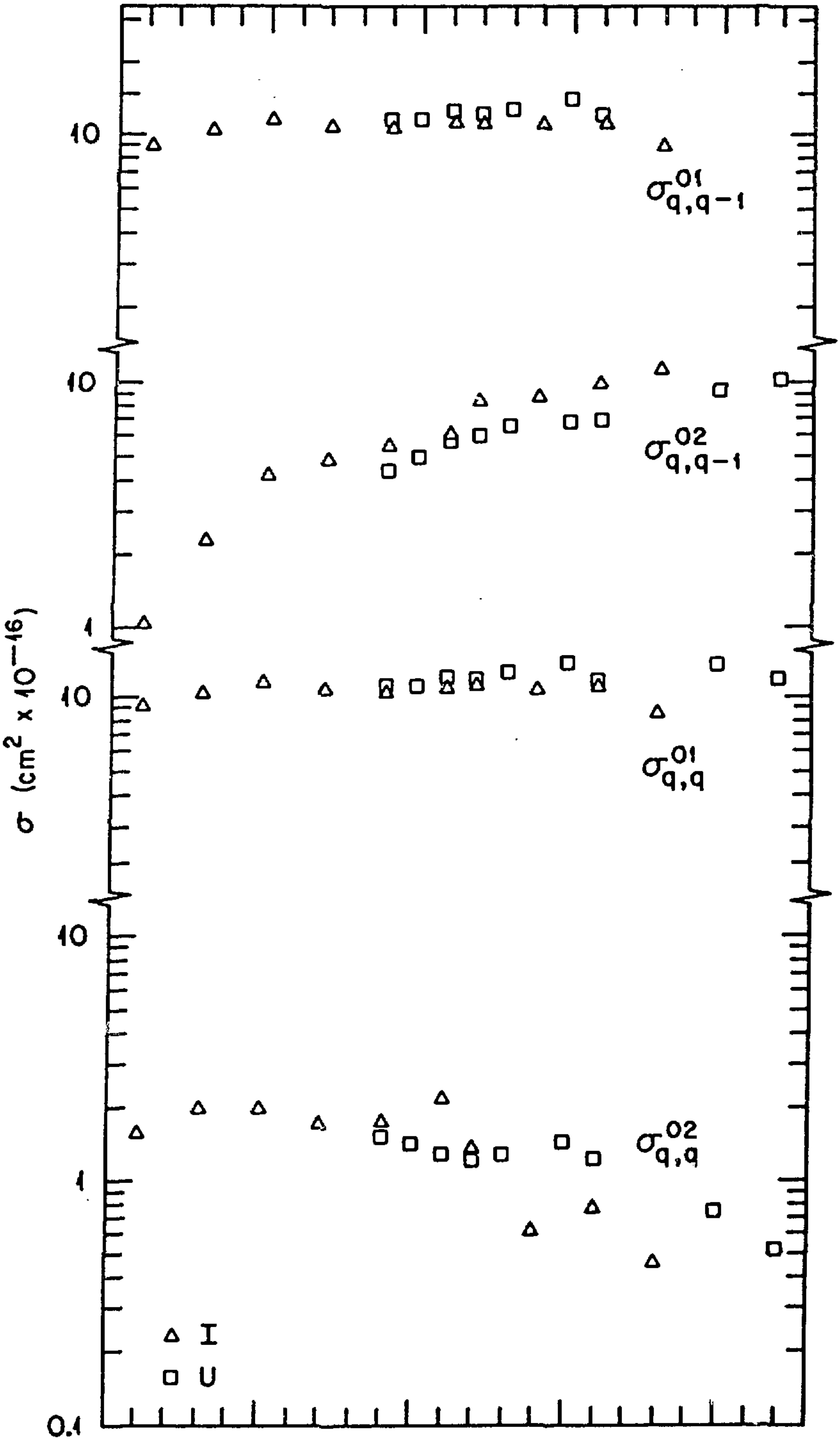

Fig. 3

ORNL—DWG 86—18499

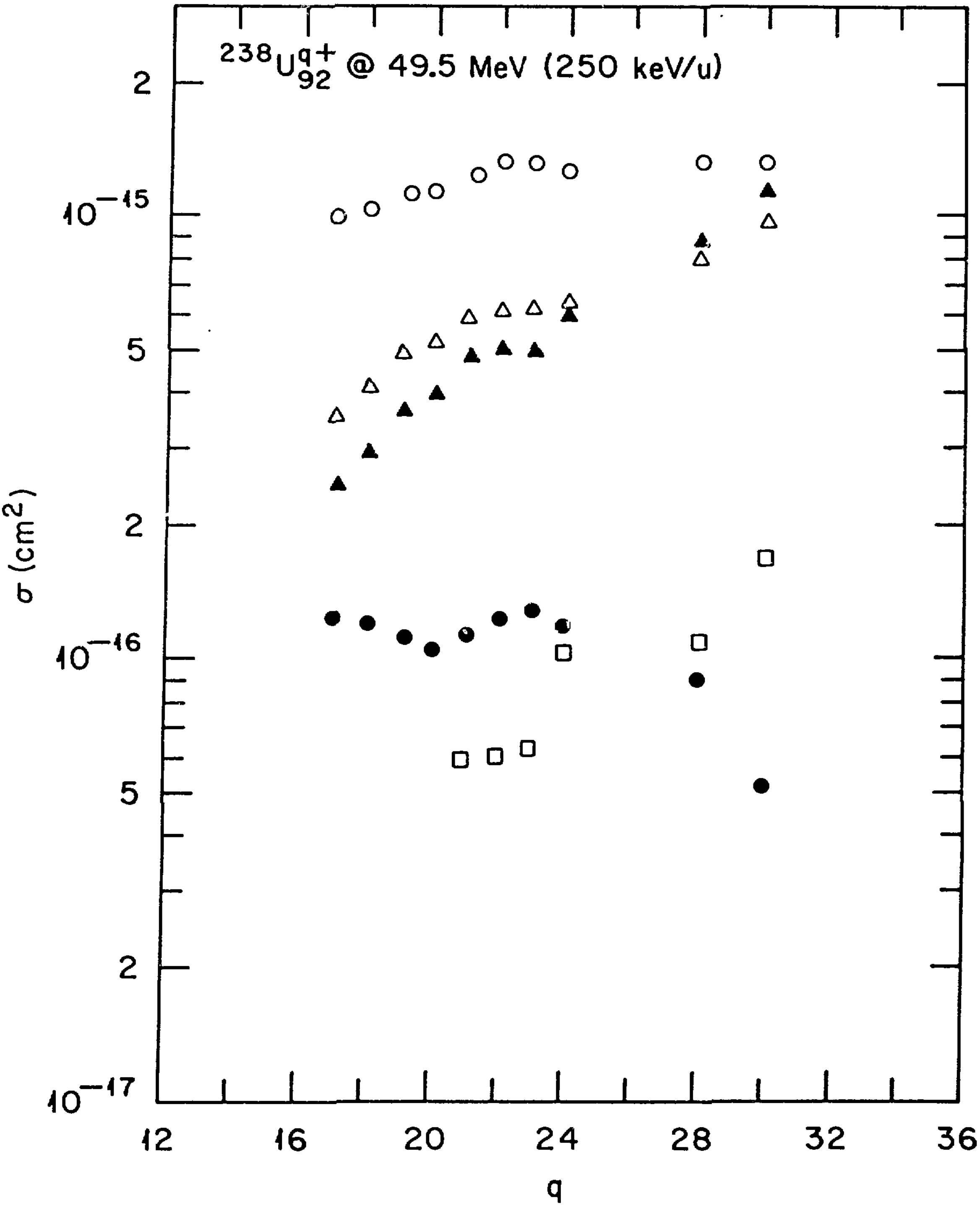

Fig. 4

ORNL-DWG 86-18197

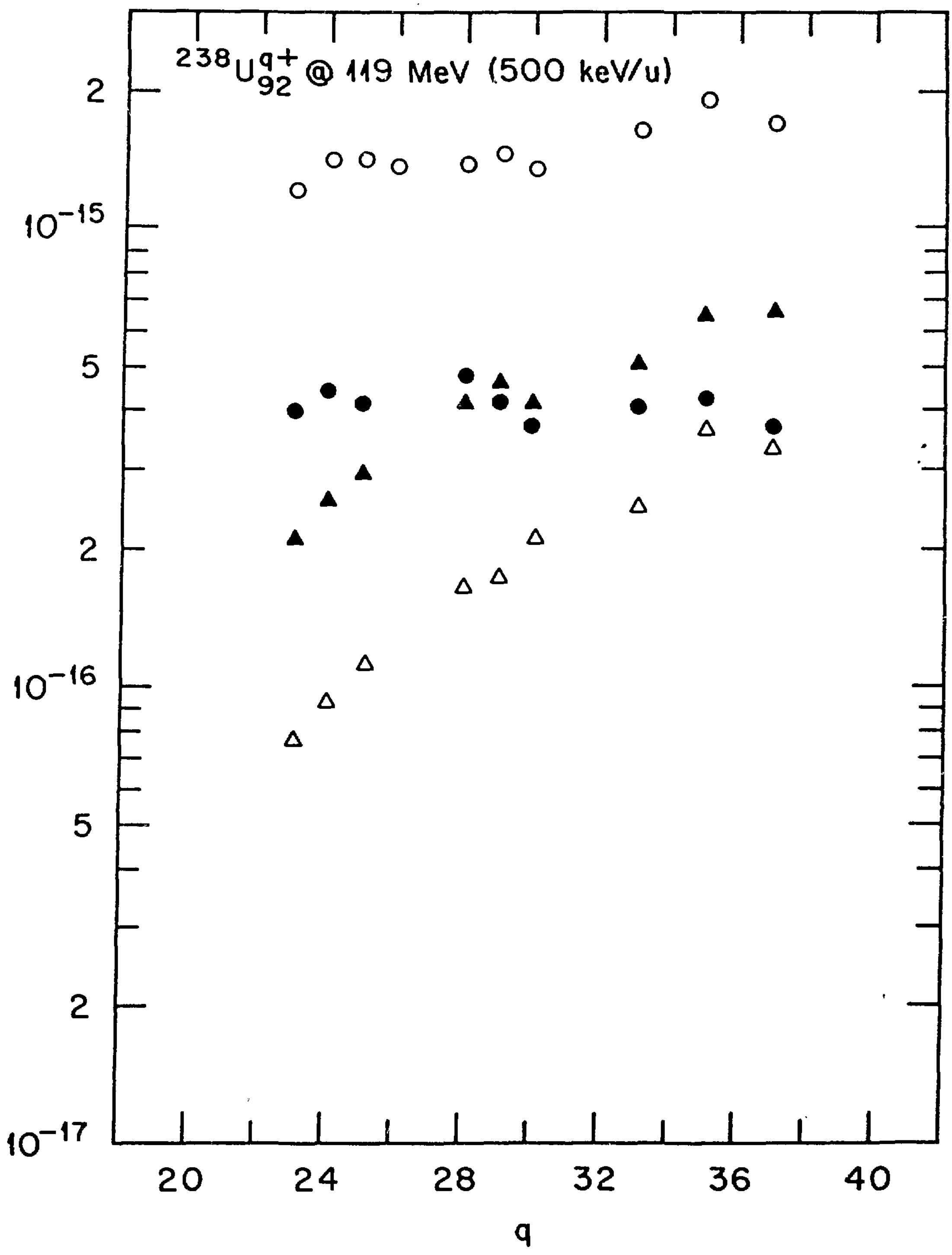

Fig. 5

ORNL—DWG 86–18198

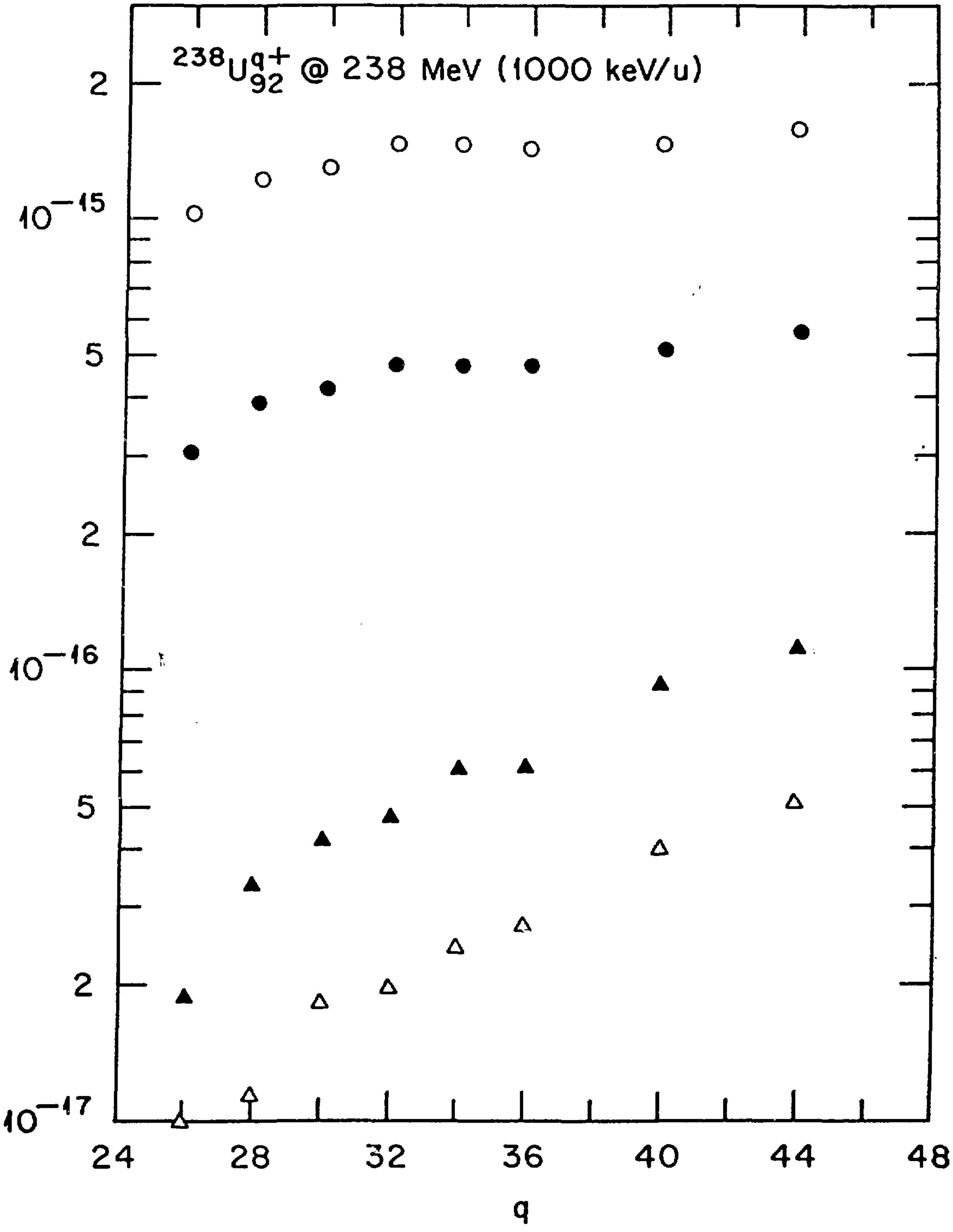

Fig. 6

ORNL–DWG 86–18204

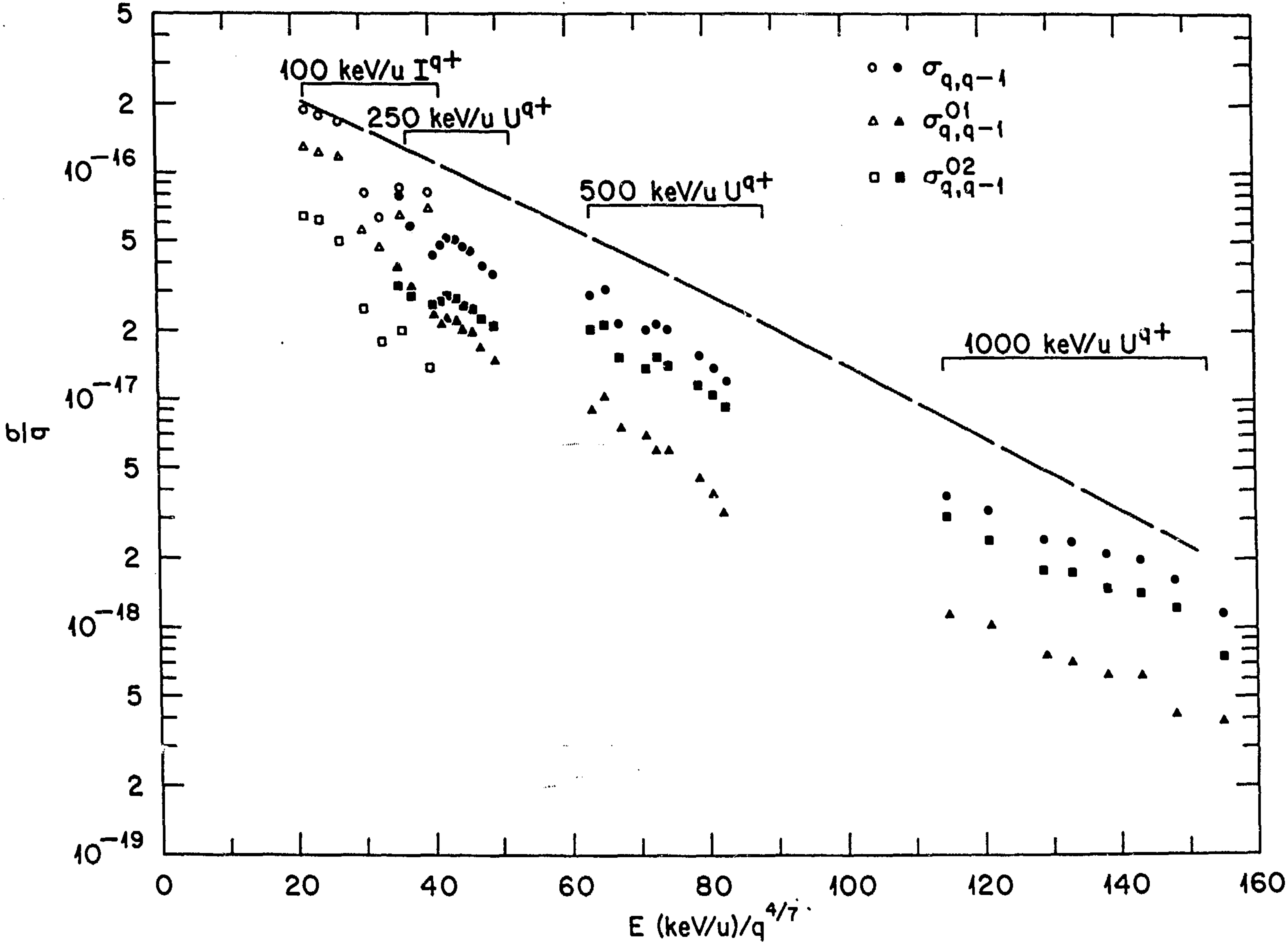

Fig. 7

ORNL—DWG 86—18200

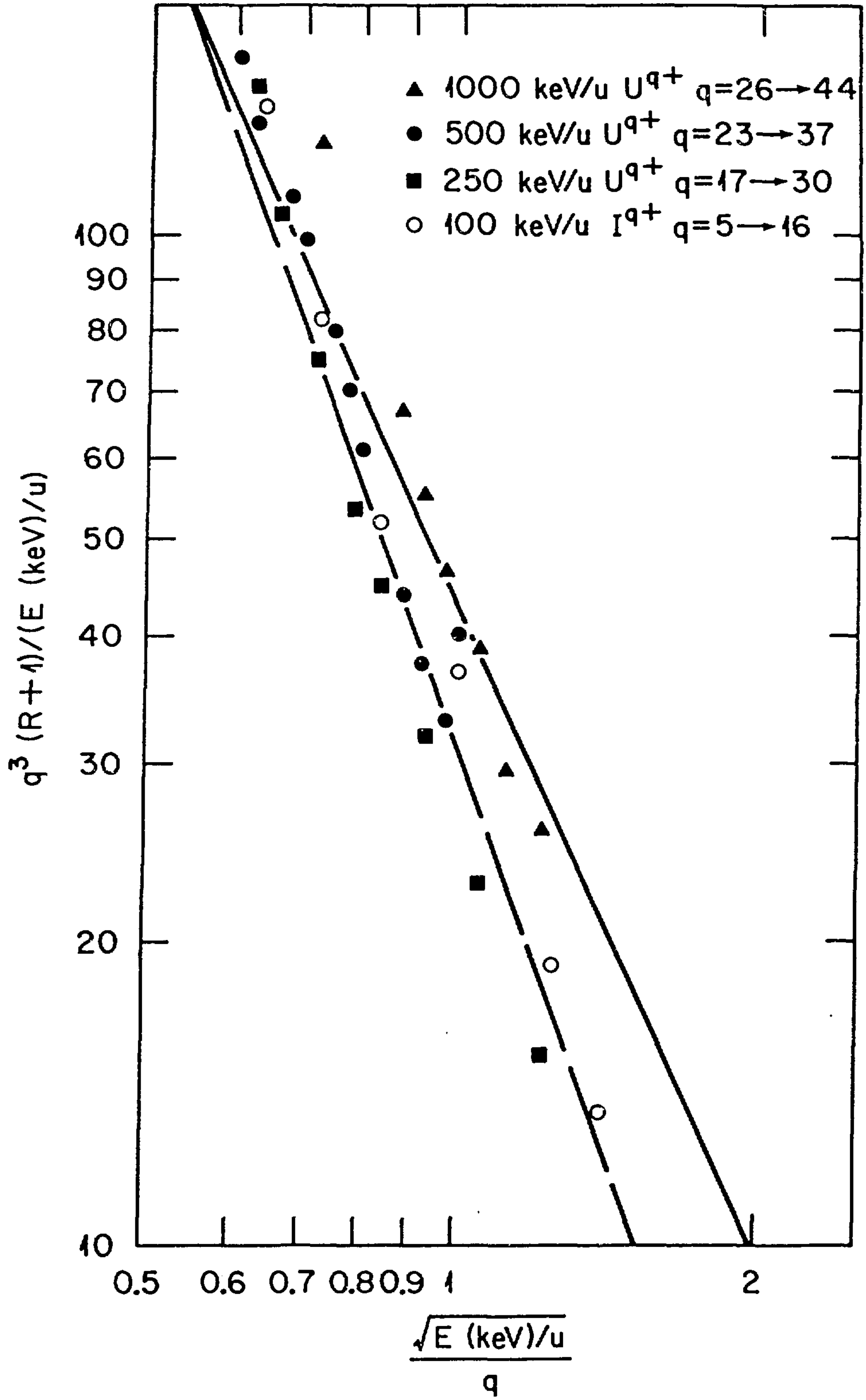

Fig. 8

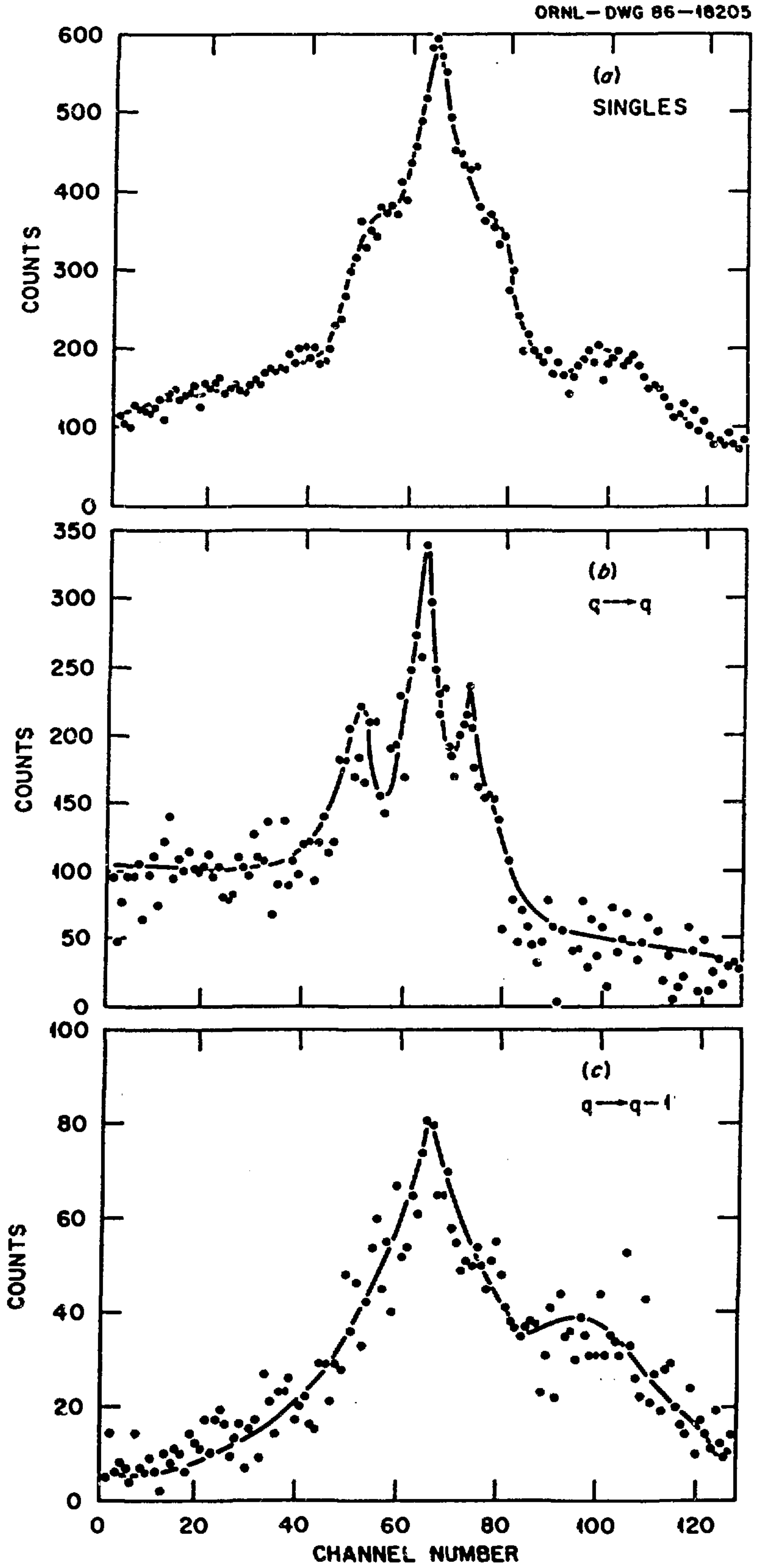
ORNL–DWG 86–18205
(a)
SINGLES
(b)
q→q
(c)
q→q–1
COUNTS
0
100
200
300
400
500
600
0
50
100
150
200
250
300
350
0
20
40
60
80
100
0
20
40
60
80
100
120
CHANNEL NUMBER

Fig. 9

ORNL-DWG 87-8408

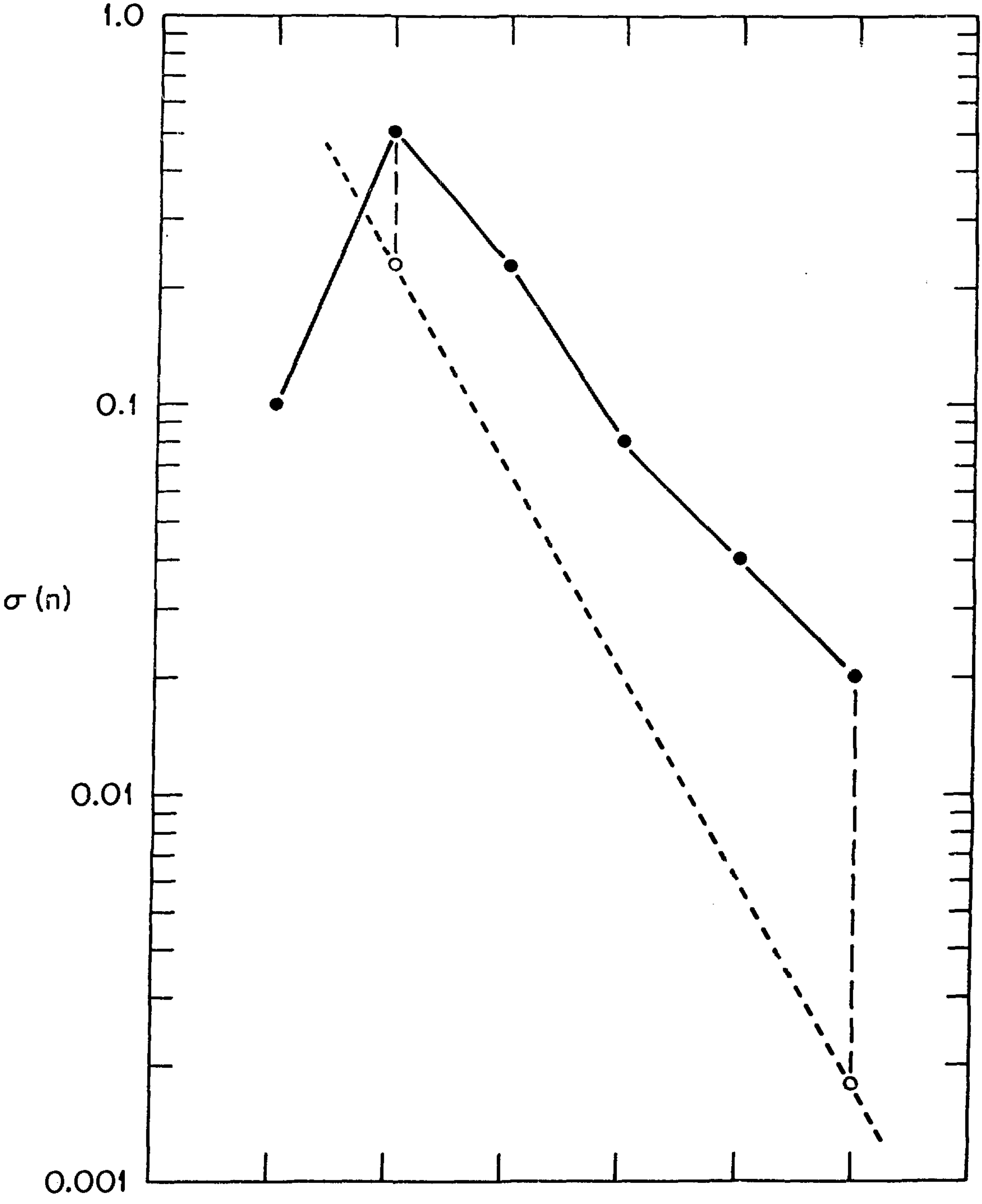

Fig. 10